KTeV Measurement of $\mathrm{Re}(\epsilon'/\epsilon)$ and Review of Recent Results on Rare Kaon Decays

Tony Barker

Department of Physics, CB 390
Boulder, Colorado, USA
Email: tonyb@cuhep.Colorado.edu

Abstract: The KTeV experiment E832 has performed a new measurement of the CP-violation parameter $\mathrm{Re}(\epsilon'/\epsilon)$ using a two-beam technique with an active regenerator. Based on about 25% of the data collected in the 1997 E832 run at Fermilab, they find $\mathrm{Re}(\epsilon'/\epsilon) = (28.0 \pm 3.0 \pm 2.8) \times 10^{-4}$, a result definitely inconsistent with zero and larger than most recent theoretical predictions. KTeV, NA48 at CERN and a number of other experiments at KEK and Brookhaven have also reported new results on a variety of rare decays of both neutral and charged kaons. Of these, the most notable is the observation of a single $K^+ \to \pi^+\nu\bar{\nu}$ event by E787 at Brookhaven. This mode and the related neutral decay $K^0_L \to \pi^0\nu\bar{\nu}$ are the primary focus of rare decay efforts planned for the medium- and long-term future.

1. KTeV Measurement of $\mathrm{Re}(\epsilon'/\epsilon)$

1.1 Definition of ϵ' and Measurement Technique

There are two neutral kaon states which are eigenstates of strangeness: $K^0 = \bar{s}d$ and $\overline{K}^0 = s\bar{d}$. The operator CP transforms these into each other, and so has two eigenstates

$$|K^0_1\rangle = \frac{1}{\sqrt{2}}\left(|K^0\rangle + |\overline{K}^0\rangle\right)$$

with $CP|K^0_1\rangle = +|K^0_1\rangle$, and

$$|K^0_2\rangle = \frac{1}{\sqrt{2}}\left(|K^0\rangle - |\overline{K}^0\rangle\right)$$

with $CP|K^0_2\rangle = -|K^0_2\rangle$. If CP were an exact symmetry of the weak interactions, these would correspond to the mass eigenstates K^0_L and K^0_S. Specifically, only the CP-even state K^0_1 would be allowed to decay to two pions, and it would therefore be identified with the K^0_S, which nearly always decays in that channel; while the CP-odd state K^0_2 would have to decay to 3π or semileptonic final states, and would therefore correspond to the longer-lived K^0_L.

Since 1964, we have known that this simple picture, in which the K^0_1 is identified with the K^0_S, and the K^0_2 with the K^0_L, is not correct. In that year, Christenson, Cronin, Fitch, and Turlay [1] found that the K^0_L has a small, but non-zero probability of decaying into two-pion final states, which implies that CP symmetry is violated. Unlike the violation of parity symmetry alone, which is maximal, CP violation is a small effect. The violation of CP in neutral kaon decays could be explained by a small CP-violating mixing between the CP eigenstates, so that the mass eigenstates would be

$$|K^0_S\rangle = \frac{1}{\sqrt{1+|\epsilon|^2}}\left(|K^0_1\rangle + \epsilon\,|K^0_2\rangle\right)$$

and

$$|K^0_L\rangle = \frac{1}{\sqrt{1+|\epsilon|^2}}\left(|K^0_2\rangle + \epsilon\,|K^0_1\rangle\right).$$

This mechanism leads to what is called *indirect* CP violation, in which the K^0_L decays to $\pi^+\pi^-$ or $\pi^0\pi^0$ final states through its small K^0_1 admixture. The probability for such decays is small because the parameter ϵ is small. Indeed, the observed rate for $K_L^0 \to \pi\pi$ can be explained if ϵ is a complex number with magnitude and phase

$$|\epsilon| = 2.269 \times 10^{-3} \qquad \phi_\epsilon = 44.3°.$$

Soon after the discovery of CP violation, it was proposed that the mixing between CP eigenstates could be a consequence of a so-called Superweak [2] interaction which would mediate CP-violating transitions with $\Delta S = 2$. Such interactions would permit $K^0 \to \overline{K}^0$ and $\overline{K}^0 \to K^0$ transitions which could lead to indirect CP violation. They could not, however, lead to CP violation in the $\Delta S = 1$ decays of the K_1^0 or K_2^0. This second type of CP violation is called *direct*. Other theories, including the Standard Model, that explain CP-violation generally have $\Delta S = 1$ effects as well as higher-order $\Delta S = 2$ effects (such as mixing). In these theories, one expects to see both direct and indirect CP violation. Indeed, it is desirable to measure both types of CP violation to provide two independent measurements of CP-violating phenomena which can be compared to the predictions of a given theory.

Direct CP violation can be distinguished from indirect by considering the balance between the two possible $\pi\pi$ final states. The K_S^0 decays to $\pi^+\pi^-$ twice as often as it does to $\pi^0\pi^0$. Since the K_S^0 is dominantly the K_1^0 eigenstate, which decays dominantly to $\pi\pi$, the ratio observed in K_S^0 decays is the ratio in K_1^0 decays. If CP violation is entirely indirect, then the K_L^0 can decay to $\pi\pi$ only through its K_1^0 component, and the ratio of charged to neutral $\pi\pi$ final states would be identical to that observed in K_S^0 decays. If, on the other hand, direct CP ciolation is also allowed, then the ratio of charged to neutral final states seen in K_L^0 decays might be altered slightly from that observed in K_S^0 decays because some of the $\pi\pi$ decays of the K_L^0 would occur directly, through its dominant K_2^0 component. To make this quantitative, one defines the amplitude ratio

$$\eta_{+-} = \frac{A(K_L^0 \to \pi^+\pi^-)}{A(K_S^0 \to \pi^+\pi^-)}$$

and its neutral counterpart

$$\eta_{00} = \frac{A(K_L^0 \to \pi^0\pi^0)}{A(K_S^0 \to \pi^0\pi^0)}.$$

If CP violation were entirely indirect, then both of these amplitude ratios would simply be equal to ϵ. If there is direct CP violation as well, then the two amplitude ratios can split apart. In particular, consider decay amplitudes for $K^0 \to \pi\pi$ in which the $\pi\pi$ state has isospin I:

$$\langle K^0 | T | \pi\pi,\ I \rangle = A_I e^{i\delta_I}.$$

Here we must have either $I = 0$ or $I = 2$, and we can choose a phase convention in which A_0 is real. The δ_I are the $\pi\pi$ final-state phase shifts. In terms of these amplitudes, a second CP violation parameter ϵ' can be defined by

$$\epsilon' = \frac{i}{\sqrt{2}}\, e^{i(\delta_2 - \delta_0)}\, \frac{\mathrm{Im}(A_2)}{A_0}.$$

This parameter describes the amount of direct CP violation in $K^0 \to \pi\pi$ decays. The splitting between η_{00} and η_{+-} is given to a good approximation by

$$\eta_{00} = \epsilon - 2\epsilon' \qquad \text{and} \qquad \eta_{+-} = \epsilon + \epsilon'.$$

To measure the splitting, experiments consider the double ratio of partial widths

$$R = \frac{\Gamma(K_L \to \pi^0\pi^0)/\Gamma(K_S \to \pi^0\pi^0)}{\Gamma(K_L \to \pi^+\pi^-)/\Gamma(K_S \to \pi^+\pi^-)}.$$

In terms of the parameters defined above, this ratio is given by

$$R = \left| \frac{\eta_{00}}{\eta_{+-}} \right|^2 = 1 - 6\,\mathrm{Re}\left(\frac{\epsilon'}{\epsilon}\right).$$

Thus, roughly speaking, one measures all four decay modes and determines whether the double ratio R differs from unity. The difference yields six times the quantity $\mathrm{Re}(\epsilon'/\epsilon)$. If the difference is significantly different from zero, then ϵ' is non-zero, and the origin of CP violation in the neutral kaon system cannot be entirely Superweak.

Predictions of $\mathrm{Re}(\epsilon'/\epsilon)$ in the Standard Model are quite difficult because of the hadronic matrix elements involved. It is currently thought that the most important contributions come from $s \to d\,g$ transitions (gluonic penguins) and $s \to d\,Z$ or $s \to d\,\gamma$ transitions (electromagnetic penguins). It appears that these two contributions interfere destructively, so that the residual value of ϵ' is especially difficult to calculate accurately. Recent

Standard Model calculations [3] of $\mathrm{Re}(\epsilon'/\epsilon)$ are generally in the range from 2×10^{-4} to 20×10^{-4}, depending on various parameters including f_K, B_K and m_s, the strange quark mass. Quite recently, it has been suggested that the value of ϵ' may be significantly enhanced by final-state interactions [4]. Given the wide range of theoretical predictions, all one can say at the moment is whether a measurement of $\mathrm{Re}(\epsilon'/\epsilon)$ falls within this fairly wide range consistent with the Standard Model; in particular, it is not yet possible to actually extract CKM matrix elements based on a measurement of $\mathrm{Re}(\epsilon'/\epsilon)$.

1.2 Overview of KTeV Experiment E832

KTeV (Kaons at the TeVatron) is a project at Fermilab encompassing two distinct experiments: E832, whose goal is a precision measurement of $\mathrm{Re}(\epsilon'/\epsilon)$; and E799, which aims to search for a wide variety of rare K_L^0 decays, particularly the modes $K_L \to \pi^0 e^+ e^-$, $K_L \to \pi^0 \mu^+ \mu^-$, and $K_L \to \pi^0 \nu\bar{\nu}$. These three modes have significant contributions from direct CP-violating electromagnetic penguin amplitudes in the Standard Model, and so have the potential to provide complementary information about Standard Model mechanisms of CP violation.

Both experiments use a mostly-new apparatus, with only a few experiment-dependent differences. The ϵ' experiment, E832, requires two parallel beams of neutral kaons. These are created by having a beam of 800 GeV protons from the TeVatron strike a BeO target. Any charged particles produced are magnetically swept from the beam, as are the charged decay products of short-lived neutrals. The resulting beam of long-lived neutral particles passes through collimators which produce two parallel beams travelling through an evacuated beampipe toward the spectrometer. Additional sweeping magnets are placed just upstream of the spectrometer to remove the decay products of particles like Λ baryons or K_S^0 mesons, which may have decayed in the beampipe. The spectrometer begins about 95 meters downstream of the target, and the two beams that reach it consist almost entirely of photons, neutrons, and K_L^0 mesons, with some few residual K_S^0, Λ, and Ξ^0 particles at the highest energies. The kaons in the beam have energies ranging up to about 200 GeV.

Since the goal of E832 is to compare K_L^0 and K_S^0 decays, the next step in E832 is to create K_S^0 particles in one of the two beams. This is done by placing a regenerator consisting of a series of plastic scintillator tiles in one of the two beams. As the kaons pass through the regenerator, the mixture of K^0 and $\overline{K}^0$, originally 50-50, changes gradually, so that the exiting beam contains a regenerated K_S^0 component in addition to an attenuated K_L^0 component. Although the regeneration amplitude is of only modest size, the K_S^0 that are produced decay quickly downstream of the regenerator and so dominate the decays in the beam in which the regenerator is placed. More precisely, the regenerator beam is a coherent superposition of K_S^0 and K_L^0 components. The distribution of decay proper times in the regenerator beam exhibits the usual interference phenomena seen in a mixed neutral kaon beam, and its detailed shape depends on parameters of the neutral kaon system such as the K_L^0-K_S^0 mass difference Δm and the K_S^0 lifetime τ_S as well as the regeneration amplitude and the CP-violating amplitude ratios η_{00} and η_{+-}. The decay distributions seen in the second (vacuum) beam, are almost pure K_L^0. The vacuum beam is used to normalise the decay distributions seen in the regenerator beam and to understand the acceptance of the apparatus. Because the two beams (left and right) are not absolutely identical in energy, size, or intensity, the regenerator alternates from one beam to the other every minute in order to average out these differences. This will also average out any left-right asymmetry in the response of the spectrometer used to detect the K^0 decay products. Since K_L^0 and K_S^0 decays are collected simultaneously, with identical event selection criteria, many possible systematic differences in the acceptance cancel out.

As the K_L^0 beam passes through the regenerator, a variety of interactions can occur in addition to coherent regeneration. For example, there can be diffractive regeneration and inelastic scattering. In these scattering processes, energy is deposited in the scintillator tiles that make up the regenerator, and scintillation light is released. The tiles are viewed by photomultiplier tubes

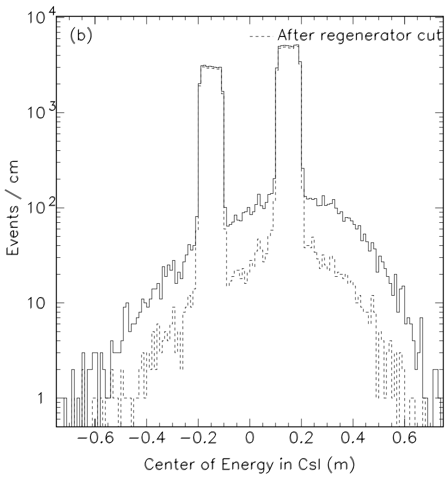

Figure 1: Center-of-energy distribution with and without active regenerator cut.

that amplify the signals. Whenever a significant signal is seen in the regenerator, the event is rejected. The fully active regenerator thus reduces the amount of background from diffractive regeneration and inelastic scattering in the regenerator material by about an order of magnitude compared to what would be observed with an opaque, passive regenerator like the one used in the previous Fermilab ϵ' experiment, E731. This reduction can be seen in figure 1, which shows the center-of-energy distribution for $K^0 \to \pi^0\pi^0$ decays. Both K_L^0 decays in the vacuum beam and the decay of coherently-regenerated K_S^0 have a center-of-energy that reflects the location of the decay vertex, and so peaks in one of the two beams. The events whose center-of-energy is outside the beam regions are background from diffractive and inelastic processes, where the decaying kaon has been scattered. The solid histogram shows the total number of these background events. The much lower dashed histogram shows the number that remain after events that deposit energy in the active regenerator have been removed from the sample.

1.3 KTeV Apparatus

The KTeV apparatus is shown in figure 2. The regenerator can be seen at the lefthand (upstream) edge of the schematic. It is preceded by a lead-scintillator "mask-anti" whose purpose is to reject any event with particles outside of the nominal beam regions; such events are usually upstream decays. After the regenerator, there is a large vacuum decay volume. The vacuum tank extends somewhat more than 30 meters downstream from the regenerator, and increases gradually in diameter from about 1.5 meters at the regenerator to about 2.0 meters just before the window at its downstream end. Every few meters along this vacuum tank, there are so-called "ring vetoes", $16X_0$ lead-scintillator stacks with a square hole in the center, labelled $RC6 - RC10$ in figure 2. The beams, as well as decay particles within the fiducial volume of the detector, pass through the square apertures. Decay products that are exiting the tank at large angles, so that they would miss the spectrometer elements further downstream, hit the veto detectors and produce a signal that causes the event to be rejected, either at trigger level or in the offline analysis. This helps to minimize backgrounds due to missing particles. The most important such background is $K_L \to \pi^0\pi^0\pi^0$ with two missing photons, which might sometimes be mistakenly reconstructed as $K_L \to \pi^0\pi^0$ were it not for the presence of the veto detectors.

At the downstream end of the vacuum tank, there is a large, thin window. Just beyond this window is the first of four multiwire proportional chambers. There are two chambers upstream of an analysis magnet ($C1$ and $C2$ in figure 2), and two more downstream of the magnet ($C3$ and $C4$). Each chamber has two horizontal and two vertical planes of sense wires, in order to locate charged tracks in both X and Y views, and to resolve the left-right ambiguities. The chambers have a resolution of about 110 microns. The analysis magnet imparted a transverse momentum kick of 412 MeV/c, allowing a momentum measurement with a resolution of about 0.5% at 50 GeV/c momentum. The drift chambers are each surrounded by additional veto detectors in order to reject events with particles escaping the fiducial volume of the detector before reaching the calorimeter. These veto detectors are labelled $SA2 - SA4$ in figure 2.

The calorimeter is used to measure the energy of photons as well as the energy deposited

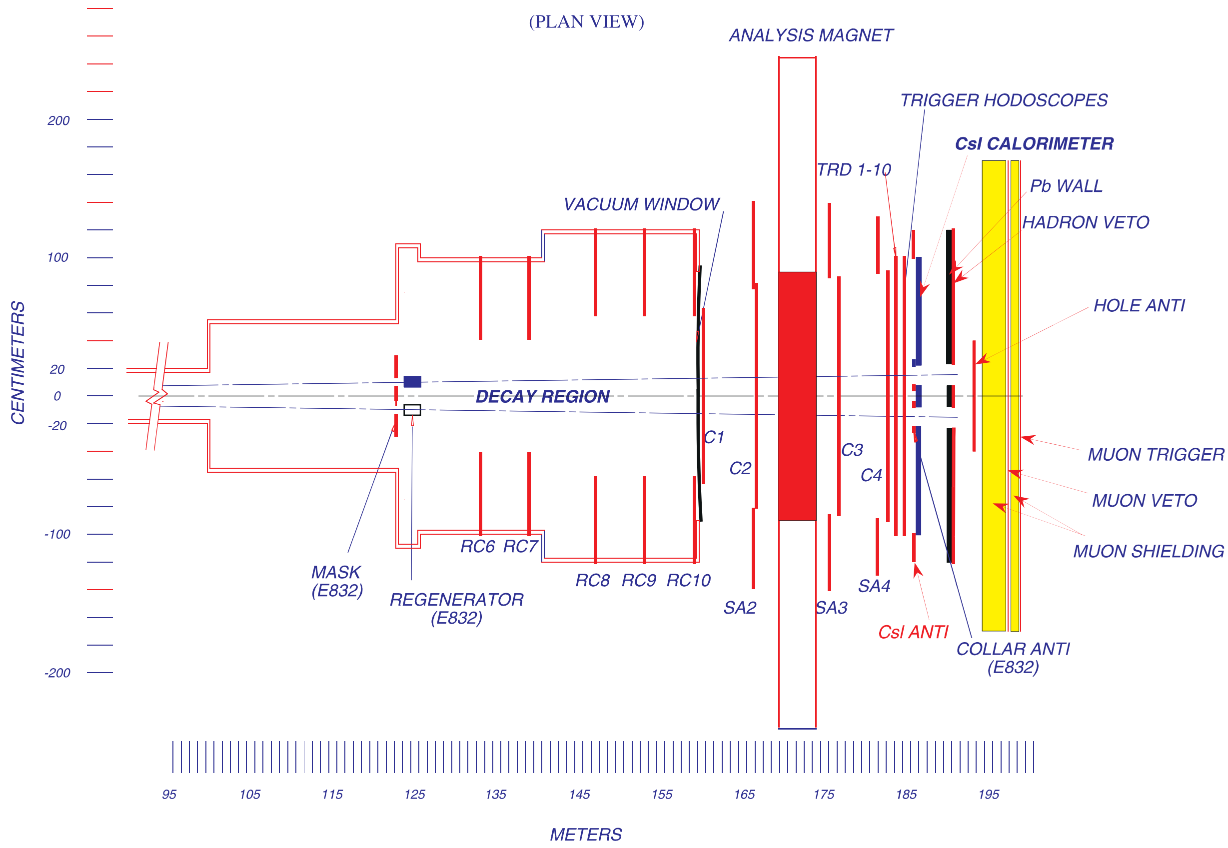

Figure 2: Schematic of KTeV apparatus. Note different horizontal and vertical scales.

by charged particles, which can be electrons, pions, or muons. It consists of 3100 crystals of pure CsI. The crystals are all 50 cm long (about $27X_0$). The crystals toward the outside of the array, far from the beams, are 5 cm by 5 cm transversely; the inner crystals are 2.5 cm by 2.5 cm. To prevent particles in the beam from interacting in the CsI, the calorimeter has two beam holes each 15 cm square where the beams pass through. A final veto detector, the CsI Anti, surrounds the outer edge of the CsI array. In addition, the inner edge of the CsI acceptance is precisely defined by a tungsten-scintillator veto detector that surrounds the edges of the two CsI beam holes.

Electrons and photons deposit all their energy in the CsI, whereas pions deposit only the minimum-ionizing energy of about 300 MeV most of the time. Thus $K^0 \to \pi^\pm e^\mp \bar{\nu}(\nu)$ (K_{e3}) events with a minimum-ionizing pion can be used as a clean source of electrons for calibration purposes. The ratio E/p, where E is the measured energy in the CsI, and p is the momentum determined from the drift chambers, can then be used to measure the resolution of the CsI calorimeter. Figure 3 shows the E/p distribution for a sample of 190 million K_{e3} electrons. As the figure shows, the resolution on E/p, including contributions from the momentum measurement in the chambers as well as the energy measurement in the CsI, averages about 0.7%; the energy resolution of the CsI varies from about 1% at 5 GeV to about 0.6% above 50 GeV. This excellent resolution is extremely important for the neutral-mode ($\pi^0\pi^0$) analysis, since the location of the decay vertex is determined entirely from the calorimeter's photon energy measurements. Good energy resolution is also important to the reduction of certain backgrounds in E799 rare decay searches.

Downstream of the CsI, there is four meters of muon filter steel, plus scintillator hodoscopes designed to detect muons. Signals in these detectors allowed us to veto decays with muons at trigger level in E832.

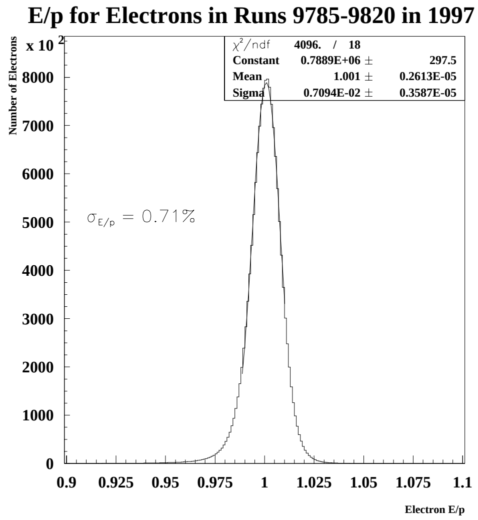

Figure 3: Distribution of E/p for 190 million electrons collected during normal KTeV running, showing the excellent energy resolution of the CsI calorimeter.

There were separate triggers for the charged and neutral $\pi\pi$ modes in E832. The charged trigger required that at least a certain minimum number of hits registered in the drift chambers, and that the hits had a spatial pattern consistent with a two-track event. Charged events also had to have at least two hits in scintillator planes just upstream of the CsI (as shown in figure 2). The neutral trigger required a significant total energy deposit in the CsI, and further that there be four or five distinct clusters of CsI crystals with energy above a 1 GeV threshold. A software-based Level 3 trigger performed a fast online event reconstruction and applied loose event selection criteria to further reduce the number of events that had to be written to tape.

Additional triggers were used to simultaneously record large samples of common K_L^0 decays such as K_{e3}, $K_L^0 \to \pi^+\pi^-\pi^0$ and $K_L^0 \to \pi^0\pi^0\pi^0$ for calibration purposes, and to study the acceptance of the apparatus offline.

1.4 Analysis Procedure

The $K^0 \to \pi^0\pi^0$ data used in the measurement described here were collected in the first run of E832 in 1996. Neutral-mode events must have exactly four energy clusters in the CsI, each with at least 3 GeV. The clusters cannot be within 7.5 cm of each other, or within 5 cm of the outer edge of the CsI. The four photon clusters can be separated into two distinct pairs in three ways. For each pair in a pairing, the hypothesis is made that the two photons came from the decay of a single π^0. The distance of the hypothetical π^0 decay from the CsI calorimeter (Δz) can then be found from the equation

$$\Delta z = \frac{\sqrt{E_1 E_2}}{M_\pi} \Delta r,$$

where M_π is the π^0 mass; E_1 and E_2 are the measured photon energies; and Δr is the transverse separation of the two photon clusters at the CsI. Two different Δz values are calculated for the two pairs in a pairing, and uncertainties on the two Δz values are estimated. A χ^2 is then formed for the hypothesis that the two Δz values are the same, as would be expected if this pairing is the "right one" and if the event is really a $K_L^0 \to \pi^0\pi^0$ decay. The pairing with the best χ^2 is chosen, and using the weighted-average Δz for that pairing, the z decay vertex is determined. Once this is done, the total invariant mass of the event can be calculated. Only events with total mass between 490 and 505 MeV/c^2 are kept in the final neutral-mode sample.

The charged-mode data collected in the 1996 run were not used in the initial E832 analysis because of some anomalous drift chamber timing effects which led to poor efficiency for the Level 3 trigger software. The Level 3 code was modified to account for this effect between the 1996 and 1997 E832 running, and 1997 charged-mode data were used for the $\pi^+\pi^-$ sample. To identify $\pi^+\pi^-$ events, events were required to have exactly two drift chamber tracks, each with momentum of 8 GeV/c or more. The tracks had to be matched to energy clusters in the CsI, and, to be sure that they were produced by pions, the E/p ratio had to be less than 0.85. The invariant mass of the two pions had to be between 488 and 508 MeV/c^2. To reject events with missing particles, a quantity called P_T was calculated by finding the component of the total of the two measured pion momenta which was perpendicular to the kaon's line of flight from target to decay vertex. Only events with $P_T^2 < 250\,\text{MeV}^2/c^2$, consistent with resolution effects, were retained in the final charged-mode data sample.

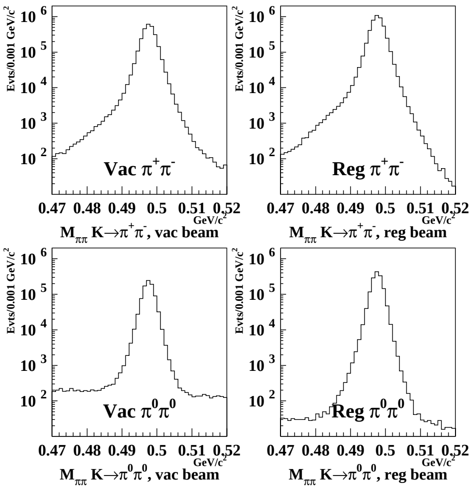

Figure 4: Distribution of invariant mass for the charged-mode and neutral-mode $K^0 \to \pi\pi$ candidate events, in both E832 beams.

After applying these selection criteria, the number of neutral-mode events found was over 0.8 million in the vacuum beam, and over 1.4 million in the regenerator beam. Some 2.6 million charged mode events were found in the vacuum beam, compared to 4.5 million in the neutral beam. The invariant mass distributions for these events are shown in figure 4.

Before $\text{Re}(\epsilon'/\epsilon)$ can be extracted from these data, backgrounds must be identified and subtracted, and acceptance corrections must be determined. Both these tasks require a Monte Carlo simulation of the experiment. The simulation models the original kaon production, the size and shape of the beams, and the geometry and response of all the detector elements. Interactions, including scattering, radiation, and pair-production are also modelled. The effect of accidental activity in the detector is taken into account by overlaying data from random events (collected, however, using a trigger whose rate is proportional to beam intensity) on top of Monte Carlo data before the reconstruction is simulated. The Monte Carlo simulation is checked by comparing a variety of distributions for high-statistics common decay modes such as $K_L^0 \to \pi^+\pi^-\pi^0$ and $K_L^0 \to \pi^0\pi^0\pi^0$, as well as for the $\pi\pi$ signal modes. The level of residual disagreement in these distributions is used to estimate the systematic errors in the final measurement.

The backgrounds to the charged mode are very small, since the P_T^2 cut is very efficient at removing them. In the vacuum beam, there is a small charged-mode background from misidentified K_{e3} and $K_{\mu 3}$ semileptonic decays, in which the lepton is misidentified as a pion. In the regenerator beam, the main background comes from regenerator scattering events. The Monte Carlo simulations of these backgrounds as a function of P_T^2 are shown in figures 5 and 6. As the figures show, the shape of the backgrounds match the data very well at large P_T^2, allowing reliable determination of the remaining background under the signal peak near zero. The level of scattering backgrounds required to match the data and Monte Carlo P_T^2 spectra can also be used to help in the determination of neutral-mode scattering backgrounds.

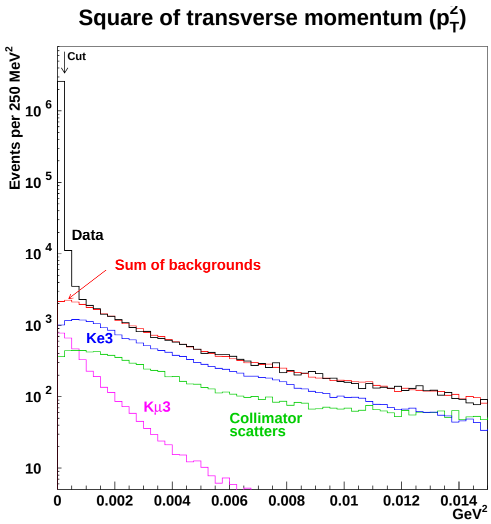

Figure 5: Distribution of P_T^2 for charged-mode candidate events in the vacuum beam, showing contributions from various backgrounds.

Because the decay vertex cannot be as precisely located in the neutral mode, there is no precise P_T^2 quantity available to reduce the backgrounds. Only a relatively crude "Ring Num-

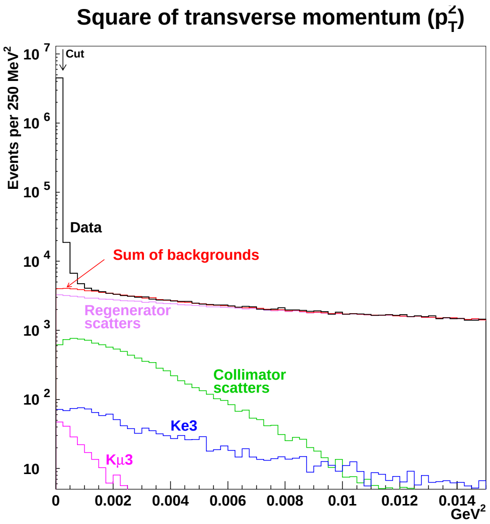

Figure 6: Distribution of P_T^2 for charged-mode candidate events in the regenerator beam, showing contributions from various backgrounds.

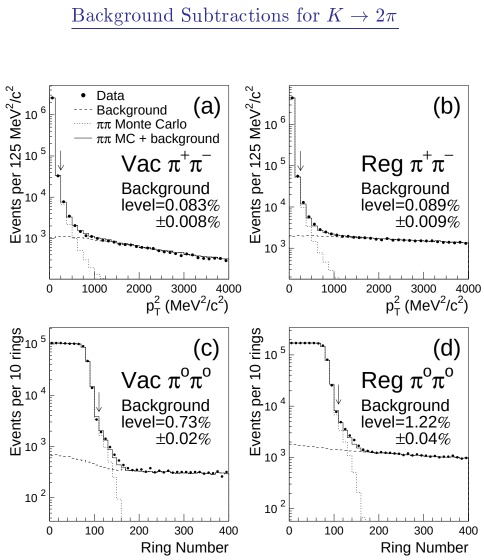

Figure 7: Summary of total background levels for all four $K_{L,S} \to \pi\pi$ modes. Shown as a function of P_T^2 for the charged mode, and of "Ring Number" (see text for definition) in the neutral mode.

ber" which is based on the center-of-energy of the four photon clusters, is available. The Ring Number is obtained by squaring the larger of the horizontal and vertical separations from the energy centroid to the center of the nearer beam. For signal events, it is required to be less than 110. Background can once again be determined by comparing the tails of the Ring Number distribution, and matching them to the sum of all the Monte Carlo background predictions. The backgrounds are substantially larger in the neutral mode, because the peak region is less tightly defined. Figure 7 shows the final background determinations for all four $K_{L,S} \to \pi\pi$ decay modes. As the figure shows, the charged-mode backgrounds are less than 0.1%, while the neutral mode backgrounds are somewhat less than 1% in the vacuum beam, and somewhat more than 1% in the regenerator beam.

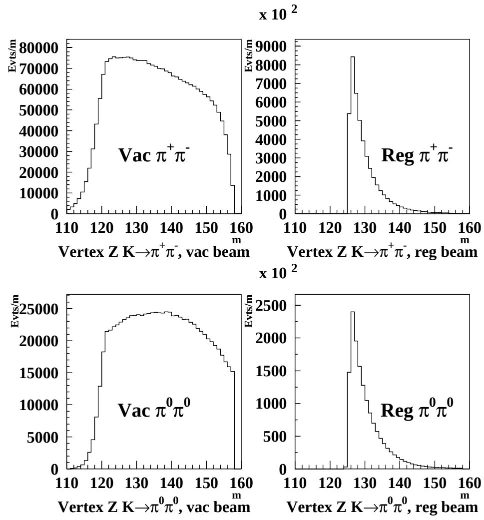

Figure 8: Background-subtracted decay-vertex distributions. Notice the sharply falling regenerator beam distributions, dominated by K_S decays, compared to the relatively flat vacuum beam distributions, dominated by K_L^0 decays.

1.5 Extraction of Re(ϵ'/ϵ)

Once the backgrounds have been determined, they are subtracted bin-by-bin from the signals, resulting in the four decay-vertex distributions shown in figure 8. The data are further divided into energy bins. In each bin of kaon energy and decay vertex position, the Monte Carlo simulation is used to determine an acceptance correction. The acceptance-corrected numbers of events are combined in 10 GeV energy bins. The ratio of regenerator to vacuum beam events is then fit to the predicted distribution, which depends on parameters including not only Re(ϵ'/ϵ), but also

Δm, τ_S, the phases ϕ_{00} and ϕ_{+-} of η_{00} and η_{+-}, and the regeneration amplitude. The fit can be done in a variety of ways, either allowing many parameters to float simultaneously, or fixing all parameters but one.

It is useful as a preliminary check to float the well-measured parameters Δm and τ_S. The results are

$$\Delta m = (0.5280 \pm 0.0013) \times 10^{10}\,\hbar\,\mathrm{s}$$

for the mass difference, and

$$\tau_S = (89.67 \pm 0.07) \times 10^{-12}\,\mathrm{s}$$

for the K_S^0 lifetime. These results are in good agreement with other precision measurements, as shown in figure 9.

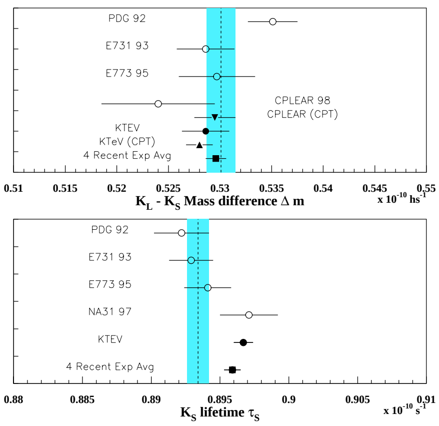

Figure 9: KTeV fit results for the K_L^0-K_S^0 mass difference Δm and the K_S^0 lifetime τ_S, compared to other high-precision measurements.

There are a variety of systematic uncertainties in the extraction of $\mathrm{Re}(\epsilon'/\epsilon)$, which are summarized in figure 10. Among the charged-mode sources of uncertainty, by far the most important is the overall acceptance uncertainty. Its origin lies in the fact the the observed z-vertex distribution in the data does not exactly match the predicted distribution in the Monte Carlo. The disagreement is at a level of about 2.5σ, a so could conceivably be statistical. However, to be conservative we assume that the disagreement represents a misunderstanding in the acceptance, and the systematic error reflects the impact such a misunderstanding would have on $\mathrm{Re}(\epsilon'/\epsilon)$.

In the neutral mode, there is no single, dominant source of systematic uncertainty. The largest single source is actually Monte Carlo statistics, which can and will be reduced through the investment of more computer time. The background uncertainty is much larger in the neutral mode simply because the level of background is about an order of magnitude larger than in the charged mode. Finally, the energy scale uncertainty is due to the fact that the calculation of the vertex location depends entirely on the overall CsI energy scale; an error in this scale would cause the whole z-vertex distribution to slide, and since this distribution is very different for K_L^0 and K_S^0 decays, such a shift would impact the fit results for $\mathrm{Re}(\epsilon'/\epsilon)$. For the final fit, all other parameters are fixed to the Particle Data Group averages, and the PDG uncertainties on those make a small contribution to the systematic error as well. Combining all the systematic errors in quadrature, the total is 2.8×10^{-4}. With this dataset, the statistical uncertainty is 3.0×10^{-4}.

Summary of Systematic Uncertainties

Systematic	$\pi^+\pi^-$ Analysis ($\times 10^{-4}$)	$\pi^0\pi^0$ Analysis ($\times 10^{-4}$)
Trigger (L1/L2/L3)	0.50	0.29
Detector Resolution	0.35	<0.10
Calibration/Alignment	0.25	0.38
Energy Scale	0.12	0.70
DC simulation	0.63	—
CsI non-linearity	—	0.60
Apertures (incl Reg Edge)	0.26	0.48
Analysis Cuts	0.59	0.78
Backgrounds	0.20	0.81
Overall Acceptance	1.59	0.68
Monte Carlo Statistics	0.50	0.90
Attenuation Slope	0.24	
Movable Absorber	0.20	
External Parameters	0.19	

Figure 10: Systematic uncertainties in the measurement of $\mathrm{Re}(\epsilon'/\epsilon)$; the largest single uncertainty is due to a mismatch between the data and Monte Carlo z-vertex distributions for the charged mode.

To avoid any bias in developing the analysis cuts or the Monte Carlo simulation based on the result for $\mathrm{Re}(\epsilon'/\epsilon)$, the fit results were "hidden" by adding an unknown offset to the reported value of $\mathrm{Re}(\epsilon'/\epsilon)$ until the decision was made to report the result in public. The final result from the fit was quite large:

$$\mathrm{Re}(\epsilon'/\epsilon) = (28.0 \pm 3.0 \pm 2.8) \times 10^{-4}.$$

As figure 11 shows, this result is considerably larger than the previous E731 result, but quite consistent with the NA31 result, as well as with the NA48 result [5]. It is also larger than most recent theoretical predictions, but as was mentioned above, the predictions are not yet well constrained considering the ranges of parameters that must be considered.

This result, together with the new results from NA48, does, however, rule out conclusively the hypothesis that the observed CP violation in neutral kaon decays might be due exclusively to a new, CP-violating Superweak interaction. Whether or not sources of CP violation beyond the Standard Model will be required to explain such a large value for $\mathrm{Re}(\epsilon'/\epsilon)$ awaits the development of more definite theoretical predictions for the CP violation induced by the CKM matrix.

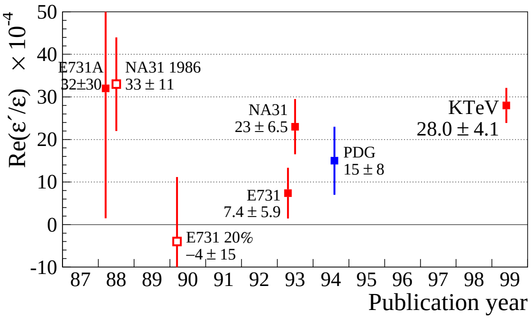

Figure 11: Final result for $\mathrm{Re}(\epsilon'/\epsilon)$, and comparison to earlier experiments. See also NA48 result [5].

2. Review of Recent Results on Rare Kaon Decays

The past two years have seen significant progress in the search for a number of rare kaon decays. In this section, I will briefly review some of the recent rare kaon decay results from a number of experiments. Given the large number of experiments working in this area, it will of course be impossible to mention every new result. For convenience, the results are organized according to experiment.

2.1 KTeV Results

The KTeV rare decay experiment E799 has already been mentioned in Section 1 of this paper. The main focus of E799 is on the three $\pi^0 l\bar{l}$ modes that are thought to have large direct CP-violating contributions in the Standard Model. The two modes with charged leptons are much easier to detect than the $\pi^0\nu\bar{\nu}$ mode, but they suffer from a number of serious difficulties. For example, there are three distinct contributions to the decay $K_L^0 \to \pi^0 e^+e^-$. One of these is the direct CP-violating amplitude discussed in Section 1. Another contribution comes from indirect CP violation, through the process $K_1^0 \to \pi^0 e^+e^-$. An accurate determination of this piece would require a measurement of the rare decay $K_S^0 \to \pi^0 e^+e^-$, which does not appear to be likely in the near future. Finally, there is a CP-conserving contribution to $K_L^0 \to \pi^0 e^+e^-$ which goes through an intermediate state consisting of $\pi^0\gamma^*\gamma^*$. Some progress has been made on determining this component from KTeV measurements [6] of the rare decay $K_L^0 \to \pi^0\gamma\gamma$ and of the related mode with one internal conversion, $K_L^0 \to \pi^0 e^+e^-\gamma$. However, there is still at least a factor of two uncertainty in the size of the CP-conserving contribution to $K_L^0 \to \pi^0 e^+e^-$.

Unfortunately, the difficulty of disentangling the three contributions to $K_L^0 \to \pi^0 e^+e^-$ is not the most serious problem in studying this mode. Like the π^0, the K_L^0 has a Dalitz decay, $K_L^0 \to e^+e^-\gamma$. At the next order in α_{QED}, the process $K_L^0 \to e^+e^-\gamma\gamma$ is encounted. As was first noted by H.Greenlee [7], there is a chance that the invariant mass of the two photons in this electromagnetic process may accidentally be close to the π^0 mass. When this happens, it is impossible to distinguish such an event from the sought-after signal $K_L^0 \to \pi^0 e^+e^-$.

E799 has looked for the radiative Dalitz process, $K_L^0 \to e^+e^-\gamma\gamma$. They have identified some 1578 events, compared to 58 events seen by an earlier phase of E799 [8] and 40 events reported by NA31. From these events, E799 has reported a preliminary branching ratio in agreement with theory. With an infrared cutoff of 5 MeV for the minimum photon energy in the K_L^0 rest frame, they find

$$B(K_L^0 \to e^+e^-\gamma\gamma) = (6.31 \pm 0.14 \pm 0.43) \times 10^{-7}$$

More importantly, the substantial statistics now available in this mode make it possible to study the various kinematic distributions, including the $\gamma\gamma$ invariant mass. Figure 12 shows the observed $M_{\gamma\gamma}$ distribution for the observed events, together with the Monte Carlo prediction for this decay. The agreement is very good, with both distributions unfortunately peaking near M_π.

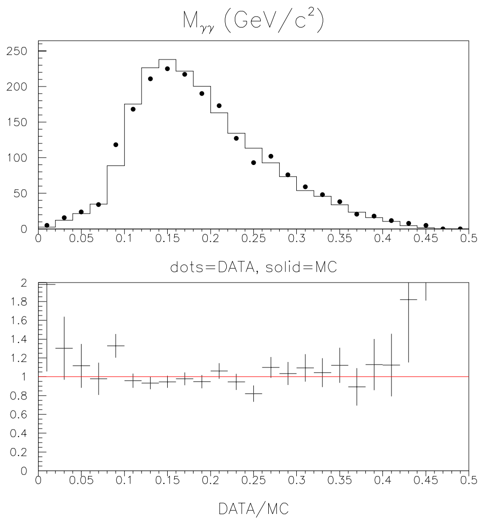

Figure 12: Observed $\gamma\gamma$ invariant mass distribution for identified $K_L^0 \to e^+e^-\gamma\gamma$ events from E799, compared to a Monte Carlo prediction. The bottom plot shows the ratio of data divided by the prediction. Events with $M_{\gamma\gamma}$ within resolution of M_π are potential background to the search for $K_L^0 \to \pi^0e^+e^-$.

The E799 group has studied these $e^+e^-\gamma\gamma$ events in order to determine an optimized set of kinematic cuts for the $K_L^0 \to \pi^0e^+e^-$ search: that is, a set of cuts that will reject as much of the $e^+e^-\gamma\gamma$ background as possible while simultaneously preserving as much of the $\pi^0e^+e^-$ signal as possible. They have found that the expected upper limit in the absence of signal is minimized if they require $\cos(\theta_\pi) < 0.746$, where θ_π is the angle between either photon momentum and the combined e^+e^- momentum, in the $\gamma\gamma$ center of momentum frame; they further require that the minimum angle between either photon and either lepton in the kaon rest frame be greater than 0.419 radians. Both of these cuts take advantage of the characteristic radiative Dalitz geometry of the $e^+e^-\gamma\gamma$ final state, in which one photon is emitted almost parallel to one lepton, and the other photon is almost back to back with the lepton pair.

With these cuts, the expected background from $K_L^0 \to e^+e^-\gamma\gamma$ to the $K_L^0 \to \pi^0e^+e^-$ search is approximately 1.5 events. Two events are observed, leading to a preliminary upper limit at the 90% confidence level:

$$B(K_L^0 \to \pi^0e^+e^-) < 5.64 \times 10^{-10}.$$

The related muonic mode $K_L^0 \to \pi^0\mu^+\mu^-$ is very similar to the $K_L^0 \to \pi^0e^+e^-$ mode, and suffers from an analogous $K_L^0 \to \mu^+\mu^-\gamma\gamma$ background. With optimized cuts, the expected background level is one event, and two are observed, leading to an upper limit

$$B(K_L^0 \to \pi^0\mu^+\mu^-) < 3.4 \times 10^{-10},$$

again at the 90% confidence level. Although the limit is slightly better than for $K_L^0 \to \pi^0e^+e^-$, the expected branching ratio is considerably smaller as well due to the reduced phase space for the muonic mode.

The most theoretically interesting of the $\pi^0l\bar{l}$ modes is $K_L^0 \to \pi^0\nu\bar{\nu}$. Unlike the two charged modes, there is no radiative Dalitz background, there is no CP-conserving contribution, and the indirect CP-violating amplitude is negligible. It is thought that the branching ratio for this mode can be predicted to better than 2%, given the CKM matrix element V_{td}. Unfortunately, this mode is extremely difficult to observe. There are no charged particles to give a decay vertex, and the two neutrinos escape the detector unobserved, leaving a single π^0. Many other kaon decays, such as $K_L^0 \to \pi^0\pi^0$ and $K_L^0 \to \pi^0\pi^0\pi^0$ can leave a single π^0 if some photons are lost. Even with highly efficient photon vetoes to prevent this, at KTeV there are processes involving hyperons, such as $\Lambda \to n\pi^0$ and $\Xi^0 \to \Lambda\pi^0$, to worry about. If the neutron or Λ escape down one of the beamholes in the CsI, this decay might also produce just a single π^0. The technique that gives the best limit at the moment involves using the Dalitz decay $\pi^0 \to e^+e^-\gamma$. This reduces the sensitivity considerably compared to the much more common $\gamma\gamma$

decay, but it allows a vertex to be found, which in turn allows the transverse momentum of the π^0 with respect to the kaon line of flight to be determined. In the $K_L^0 \to \pi^0\nu\bar{\nu}$ decay, the kinematic limit on this transverse momentum is very high, and a cut can be made which excludes all backgrounds except for $K_L^0 \to \pi^0\pi^0$, which is small enough that it can be adequately controlled using photon vetoes. The result of this search is shown in figure 13. No events are seen in the high-P_T search region, leading to a limit at the 90% confidence level

$$B(K_L^0 \to \pi^0\nu\bar{\nu}) < 5.9 \times 10^{-7}.$$

Unfortunately, the Standard Model prediction for this mode is a few times 10^{-11}, so there is a very long way to go before it can be used to extract CKM matrix elements.

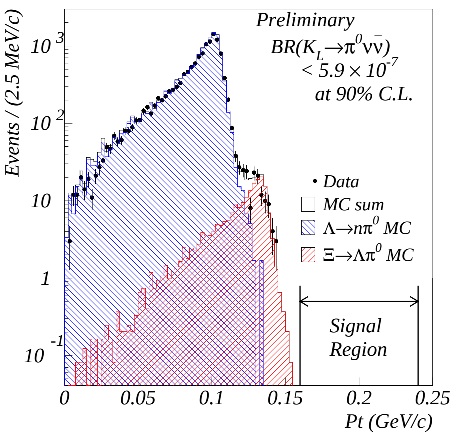

Figure 13: Distribution of π^0 transverse momentum in events where a single $e^+e^-\gamma$ having the π^0 mass is observed. The main backgrounds are from hyperon decays and are excluded by the cut shown. No events are seen in the signal region, but the sensitivity is rather poor due to the requirement of a Dalitz decay.

2.2 NA48 Results

The NA48 detector at CERN was designed to make a precision measurement of Re(ϵ'/ϵ). The details of the apparatus, and the Re(ϵ'/ϵ) analysis, are described in the contribution by Dr.P.Lubrano to these Proceedings [5]. The apparatus features an extremely large and highly precise liquid krypton calorimeter.

In addition to their measurement of Re(ϵ'/ϵ), the NA48 group have reported a number of preliminary results on rare kaon decays. They have searched for the Dalitz decay $K_L^0 \to e^+e^-\gamma$, and have observed over 6800 events in their 1997 dataset. The largest numbers observed previously were 1053 by NA31, the predecessor to NA48, and 919 by Brookhaven E845. Those two experiments obtained almost the same branching ratio, with an average of $(9.1 \pm 0.5) \times 10^{-6}$. The new, higher-statistics NA48 measurement is considerably larger. Their preliminary result is

$$B(K_L^0 \to e^+e^-\gamma) = (10.5 \pm 0.2 \pm 0.4) \times 10^{-6},$$

which disagrees at the 2σ level with the earlier measurements. They have also fit for the Bergström-Mass'o-Singer form factor parameter α_{K^*} and obtained a results consistent with previous measurements, but somewhat more precise:

$$\alpha_{K^*} = -0.36 \pm 0.06 \pm 0.02.$$

The NA48 group has also reported the observation of 84 events in the $K_L^0 \to e^+e^-e^+e^-$ channel, where they have studied the famous angular correlation in the ϕ angle between the planes formed by the two lepton pairs. The angular distribution they see is consistent with the expectation for a CP-odd state.

NA48 has also searched for the radiative Dalitz decay, $K_L^0 \to e^+e^-\gamma\gamma$. They have identified a sample of about 500 events, from which they extract a preliminary branching ratio consistent with the one reported by FNAL E799:

$$B(K_L^0 \to e^+e^-\gamma\gamma) = (5.82 \pm 0.27 \pm 0.45 \pm 0.16) \times 10^{-7},$$

with the usual infrared cutoff of 5 MeV minmum photon energy in the K_L^0 rest frame.

2.3 BNL E871 Results

Brookhaven E871 is an experiment whose main purpose is the search for the exotic lepton-flavour-violating decay $K_L^0 \to \mu^\pm e^\mp$. This decay is of course utterly forbidden in the Standard Model, but is expected in a variety of extensions such as Technicolour, theories with leptoquarks or horizontal gauge bosons, and some supersymmetric grand unified theories. Because the decay is completely forbidden in the Standard Model, the observation of even one non-background event would constitute clear evidence for new physics. If the new vector bosons coupled to quarks with the same strength as the familiar electroweak gauge bosons, then branching ratios for $K_L^0 \to \mu e$ as large as 10^{-12} or even 10^{-11} would be expected for gauge boson masses of 100 TeV, providing mass reach substantially beyond what will be directly observable even at the LHC.

BNL E871 uses K_L^0 decays in flight. Their spectrometer and trigger are optimized for two-body charged decays, including allowed modes like $K_L^0 \to \mu^+\mu^-$ and $K_L^0 \to e^+e^-$ as well as the exotic μe modes. To eliminate backgrounds to the greatest extent possible, BNL E871 relies on redundant measurements whenever possible. For example, two independent momentum measurements are made using two analysis magnets; also, two independent types of particle identification are provided for both electron-pion and pion-muon separation.

A particularly remarkable achievement of BNL E871 is that they have successfully placed a beam-plug right in the center of their spectrometer, where it has not only absorbed the beam, but has significantly reduced a variety of backgrounds.

In the $K_L^0 \to \mu^+\mu^-$ channel, E871 has observed some 6200 events, almost an order of magnitude improvement over the predecessor experiment E791. Based on this new larger sample, they have measured the branching ratio and obtained the result

$$B(K_L^0 \to \mu^+\mu^-) = (7.18 \pm 0.17) \times 10^{-9},$$

which is a notable degree of precision for such a rare decay. This decay was originally of interest because of the hope that its short-distance amplitude, which is related to V_{td} in the CKM matrix, could be extracted. However, the present measurement is extremely close to the unitarity limit, and subtracting the long-distance contribution from the $\gamma^*\gamma^*$ intermediate state to sufficient accuracy to determine the short-distance contributions now appears to be very difficult.

The decay $K_L^0 \to e^+e^-$ is exactly the same as the dimuon mode, except that it is helicity-suppressed as well as GIM-suppressed. E871 is the first experiment ever to see this decay; they have found four events and measured a branching ratio

$$B(K_L^0 \to e^+e^-) = (8.7^{+5.7}_{-4.1}) \times 10^{-12},$$

which makes this the rarest decay ever detected.

Finally, in the forbidden $K_L^0 \to \mu^\pm e^\mp$ channel, E871 has seen no events, from which they have extracted an upper limit

$$B(K_L^0 \to \mu^\pm e^\mp) < 4.7 \times 10^{-12}$$

at the 90% confidence level. Further progress in this search appears quite challenging due to the presence of backgrounds just beyond the present sensitivity.

2.4 BNL E865 Results

This experiment also searched for exotic lepton-flavour-violating decays, namely $K^+ \to \pi^+\mu^+e^-$. These decays, with an extra pion in the final state, are sensitive to exotic gauge bosons with different quantum numbers than those that could be detected in BNL E871. The experiment uses K^+ decays in flight, and the detector philosophy is similar to that of E871, with two magnets for redundant momentum measurements, and particle identification by both Čerenkov detectors and a muon range stack.

In addition to the exotic decays, BNL E865 has search for the allowed decays $K^+ \to \pi^+e^+e^-$ and $K^+ \to \pi^+\mu^+\mu^-$. In the electronic mode, they have a very large data sample of over 10,000 events, from which they have extracted a preliminary branching ratio

$$B(K^+ \to \pi^+e^+e^-) = (2.82 \pm 0.04 \pm 0.07) \times 10^{-7}.$$

They have also made a detailed study of the M_{ee} spectrum in this final state, in order to extract certain chiral perturbation theory parameters.

E865 has also observed the rarer muonic mode, with a sample of about 400 events collected in 1995. The branching ratio they have extracted is

$$B(K^+ \to \pi^+\mu^+\mu^-) = (9.2 \pm 0.6 \pm 0.6) \times 10^{-8}.$$

Finally, they have searched for, but not found, the exotic $\pi\mu e$ mode. Combining the 1995 and 1996 E865 datasets, they have reported an upper limit at the 90% confidence level:

$$B(K^+ \to \pi^+\mu^+e^-) = 3.2 \times 10^{-11}.$$

2.5 Searches for Time Reversal Violation

At KEK, a new experiment called E246 has just started running. They are using an innovative technique to look for a transverse muon polarisation in the decay $K^+ \to \pi^0 \mu^+ \nu_\mu$. The polarisation is measured by stopping the muon and using the analysing power of the electron produced in the muon decay. A transverse polarisation, out of the decay plane, would be CP-violating and T-odd. Although such effects are expected in the Standard Model due to final state interactions, as well as the usual CKM-matrix CP and T-violation, the Standard Model effects are expected to be vanishingly small: of order one part per million. KEK E246 hopes to obtain a sensitivity of about 10^{-3}. As yet, only a small amount of the planned running has taken place; so far, the collaboration report a preliminary upper limit of 0.011 on the magnitude of the transverse polarisation.

In another approach, both KTeV and NA48 have reported observing a CP-violating and T-odd angular asymmetry in the rare decay $K_L^0 \to \pi^+\pi^-e^+e^-$. This unusual effect is thought to be due to the interference between a CP-violating $K_L^0 \to \pi^+\pi^-$ amplitude with inner bremsstrahlung and internal conversion, and a CP-conserving photon direct emission amplitude, also with internal conversion of the photon. Without the internal conversion in both cases, these two amplitudes for the decay $K_L^0 \to \pi^+\pi^-\gamma$ would interfere, producing a CP- and T-violating photon polarisation. Of course, high-energy spectrometers are not capable of observing such a photon polarisation, but if the photon internally converts, the angular distribution of the e^+e^- pair created in the conversion preserves information about the photon polarisation.

The effect, predicted in 1992 by Sehgal and Wanninger [9] is an asymmetry in the distribution of the angle ϕ between the two planes formed by the lepton momenta and the pion momenta in the K_L^0 rest frame. The predicted asymmetry is quite large due to the fact the the two interfering amplitudes are of comparable size. Despite the large expected asymmetry, a signal of some hundreds of events would still be needed to see it, and prior to 1998, no observation of this mode had ever been published. In view of this, it is rather remarkable that both NA48 and FNAL E799 have now seen enough $K_L^0 \to \pi^+\pi^-e^+e^-$ events to clearly observe the expected asymmetry.

NA48 reports a signal of 458 events, over 37 background. They have reported a preliminary branching ratio

$$B(K_L^0 \to \pi^+\pi^-e^+e^-) = (2.90 \pm 0.15) \times 10^{-7}.$$

KTeV published a branching ratio [10] in 1998 based on a small subset of their 1997 data. They have now reported a preliminary branching ratio based on the full 1997 dataset, containing over 1800 events. They find

$$B(K_L^0 \to \pi^+\pi^-e^+e^-) = (3.63 \pm 0.11 \pm 0.14) \times 10^{-7}.$$

The branching ratio is larger than the one reported by NA48, but the KTeV measurement takes into account an M1 form factor which is not used in the NA48 analysis, and which significantly increases the result because it reduces the acceptance. Figure 14 shows the invariant mass spectrum observed by E799:

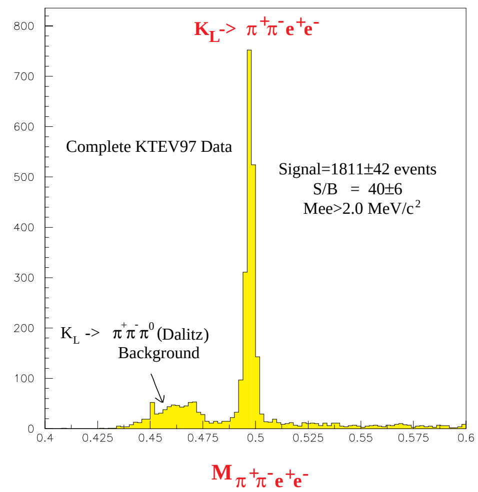

Figure 14: Distribution of invariant mass for $\pi^+\pi^-e^+e^-$ events observed by FNAL E799.

Both experiments observe a very large CP-violating and T-odd asymmetry. The asymmetry is defined by

$$A_\phi = \frac{N(\sin\phi\cos\phi > 0) - N(\sin\phi\cos\phi < 0)}{N(\sin\phi\cos\phi > 0) + N(\sin\phi\cos\phi < 0)}.$$

It is important to note that the raw asymmetry may be significantly different from the acceptance-corrected asymmetry. This occurs not because of any asymmetry in the detectors, but because the asymmetry varies across the phase space for the $\pi^+\pi^-e^+e^-$ final state, and in general there is better acceptance in regions of the phase space where the asymmetry is large than there is where it is small. The raw asymmetries observed by the two experiments are therefore not directly comparable. Nevertheless, they agree. NA48 finds $A_\phi(\text{raw}) = (20 \pm 5)\%$ while KTeV sees $A_\phi(\text{raw}) = (23.3 \pm 2.3)\%$. The angular distribution observed by FNAL E799 is shown in figure 15.

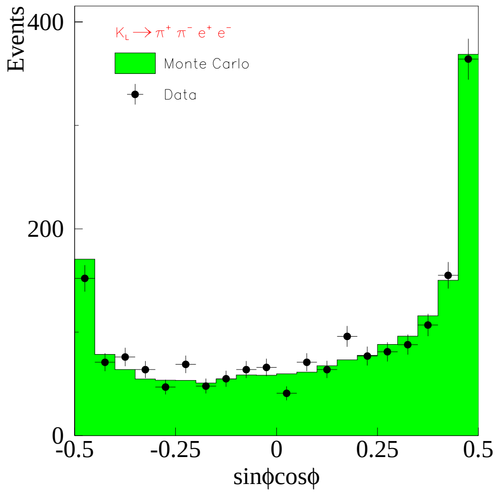

Figure 15: Distribution of the angle ϕ between the e^+e^- and $\pi^+\pi^-$ planes in the K_L^0 rest frame observed by FNAL E799. The asymmetry observed between negative and positive values of $\sin\phi\cos\phi$ is CP-violating and T-odd.

So far only KTeV has reported an acceptance-corrected asymmetry. An important ingredient in making the acceptance correction was the form factor in the M1 direct emission amplitude, which was extracted by fitting the $M_{\pi\pi}$ and other kinematic distributions. Using the fitted form factor, the acceptance corrected average asymmetry was found to be

$$A_\phi(\text{corrected}) = (13.6 \pm 2.5 \pm 1.2)\%,$$

in excellent agreement with the theoretical prediction based on the value of the indirect *CP*-violation parameter η_{+-} and the known $\pi\pi$ phase shifts.

2.6 BNL E787 Results

Brookhaven experiment E787 is dedicated to the search for the rare decay $K^+ \rightarrow \pi^+\nu\bar{\nu}$, with a sensitivity goal of better than 10^{-10}. This is one of the "golden" rare kaon decays, being related in a well-understood way to the fundamental CKM matrix elements of the Standard Model, particularly V_{td}. Like the neutral mode $K^0 \rightarrow \pi^0\nu\bar{\nu}$ discussed above, the $\pi^+\nu\bar{\nu}$ decay is expected to be quite rare, with a predicted branching ratio of less than 10^{-10}. It is also difficult to see, though less so than the neutral mode because the initial-state charged kaon and the final-state charged pion can be followed in tracking detectors.

E787 has adopted the somewhat unusual technique of using an active target to stop some of the kaons in a low-energy charged kaon beam. The stopped kaons decay, and the experiment looks for decays of the form π^+ + "nothing". Because the kaons decay from rest, the detector elements surround the target much like the components of a collider detector surround the interaction point. The detector is shown in figure 16.

A particularly dangerous background comes from the common decay $K^+ \rightarrow \pi^+\pi^0$, where the photons from the π^0 decay are lost. To eliminate this background, the experiment so far has searched for charged pions whose momentum is above the unique momentum of π^+ produced in $K^+ \rightarrow \pi^+\pi^0$ events. In the future, they hope to also use events below the $K_{\pi 2}$ peak, but this will require increased reliance on their photon detector systems, which include CsI, lead-glass, and lead-scintillator systems.

To be sure that the single charged particle apparently produced in a decay is a charged pion, the E787 detector is extensively instrumented with 500 MHz transient digitizers that give a detailed record in time of the $K^+ \rightarrow \pi^+ \rightarrow \mu^+ \rightarrow e^+$ decay chain. As with the other Brookhaven experiments, redundancy of measurement techniques is emphasized. Complementary data samples that fail some cut are frequently used to study the efficiency of other, independent cuts without "peeking" in the signal region. To keep the cuts unbiased, all cuts are finalized and expected backgrounds are determined before any data in the signal region are examined. The E787 group chose cuts that led to an expected background of about 0.07 events, so that the observation of even a single event would constitute evidence for a signal.

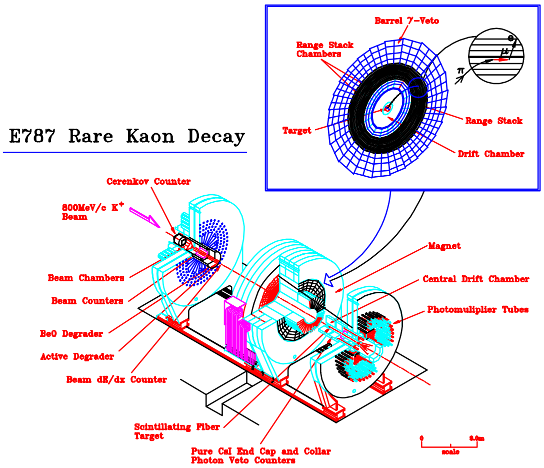

Figure 16: Drawing of the E787 stopped-kaon detector.

In the data collected in 1995, a single, clean signal event was seen, corresponding [11] to a rather large (but very uncertain) branching ratio of

$$B(K^+ \to \pi^+ \nu\bar{\nu}) = (4.2^{+9.7}_{-3.5}) \times 10^{-10}.$$

The central value is larger than could be accommodated in the Standard Model, but more data are clearly needed to draw any meaningful conclusions. Additional data collected in 1997 have been analysed, and the preliminary indication is that no additional events have been found, despite a factor 2–3 increase in sensitivity. If this holds up, the central value of the branching ratio will drop by a factor of 2–3 to a less surprising value. In 1998, additional data were collected that are alone equal to twice the combined 1995–97 sensitivity. The analysis of those data is just underway, but the results will clearly be worth waiting for, as this experiment pushes its sensitivity well into the Standard Model range.

2.7 Rare Decay Conclusions

As the preceding quick tour of the various rare kaon decay experiments at Brookhaven, Fermilab, CERN, and KEK has shown, there has been major progress on a variety of fronts in the last few years. Many of the experiments, especially BNL E787, FNAL E799, and CERN NA48, have very large quantities of data already collected but as yet not analysed, which virtually guarantees further significant progress in the short term.

The longer-term future of rare kaon decays remains bright. The KLOE detector at the DAPHNE Φ factory will soon begin to produce rare decay results on a variety of modes, and especially on K_S decays, which are as yet relatively unknown. Future efforts at Brookhaven and Fermilab are aimed squarely at the theoretically clean $K \to \pi\nu\bar{\nu}$ modes, where much can be learned about CP-violation in the Standard Model that will be complementary to the ongoing B-factory experiments. E787 and its successor experiment E949 are already probing the Standard Model sensitivity range in the K^+ decay; serious efforts are underway to attack the K_L^0 decay, but several orders of magnitude in sensitivity still stand between the current state of the art and the Standard Model predictions.

References

[1] J.H.Cristenson, J.W.Cronin, V.L.Fitch, and R.Turlay, *Phys. Rev. Lett.* **13** (1964) 148.

[2] L.Wolfenstein, *Phys. Rev. Lett.* **13** (1964) 562.

[3] M.Ciuchini, *Nucl. Phys.* **59** *(Proc. Suppl.)* (1997) 149;
A.J.Buras, `hep-ph/9806471`;
S.Bertolini *et al.*, *Nucl. Phys.* **B 514** (1998) 93.

[4] E.Pallante and A.Pich, `hep-ph/9911233`.

[5] P.Lubrano, these proceedings.

[6] A.Alavi-Harati *et al.*, *Phys. Rev. Lett.* **83** (1999) 917.

[7] H. Greenlee, *Phys. Rev.* **D 42** (1990) 3724.

[8] T.Nakaya *et al.*, *Phys. Rev. Lett.* **73** (1994) 2169.

[9] L.M.Sehgal and M.Wanninger, *Phys. Rev.* **D 46** (1992) 1035;
(e)*Phys. Rev.* **D 46** (1992) 5209.

[10] J.Adams *et al.*, *Phys. Rev. Lett.* **80** (1998) 4123.

[11] S.Adler *et al.*, *Phys. Rev. Lett.* **79** (1997) 2204.